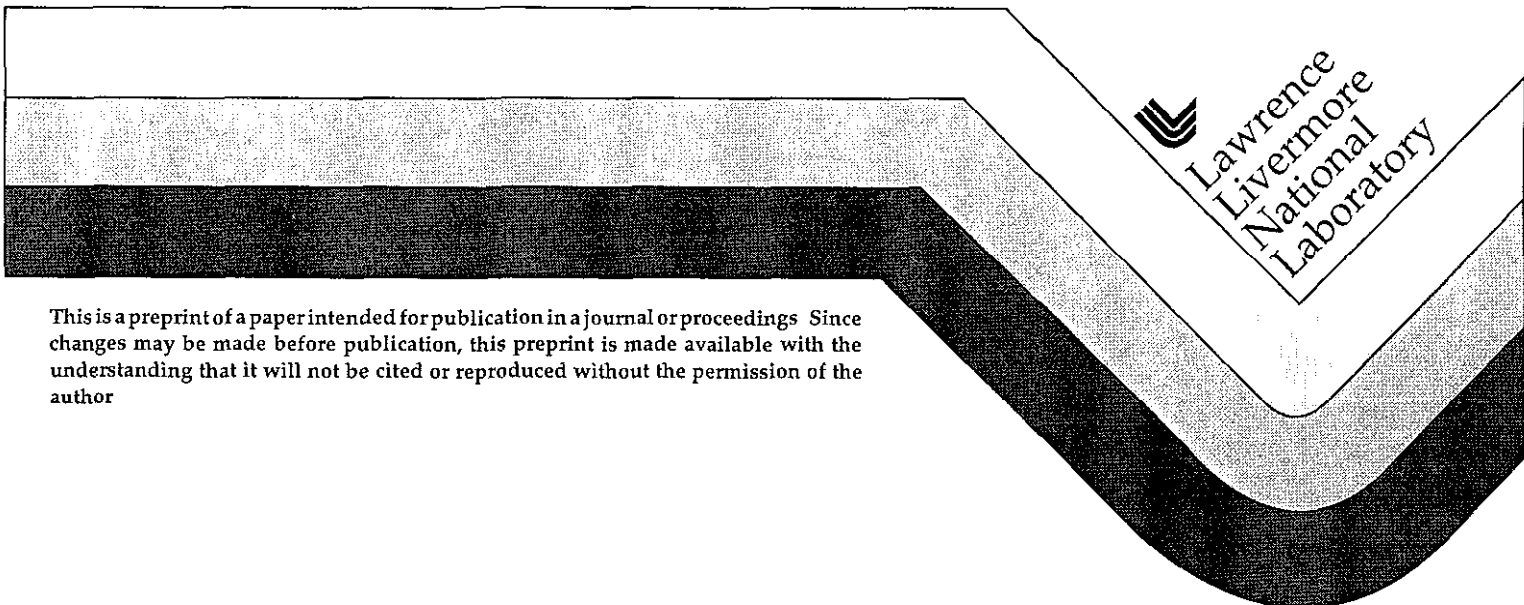


Femtosecond Laser Materials Processing

B. C. Stuart, P. S. Banks, M. D. Perry, M. D. Feit, R. S. Lee,
F. Roeske, J. P. Armstrong, H. T. Nguyen, J. A. Sefcik

This paper was prepared for submittal to the
Commercial Applications of Ultrafast Lasers
San Jose, CA
January 24-30, 1998

June 2, 1998



This is a preprint of a paper intended for publication in a journal or proceedings. Since changes may be made before publication, this preprint is made available with the understanding that it will not be cited or reproduced without the permission of the author.

DISCLAIMER

This document was prepared as an account of work sponsored by an agency of the United States Government. Neither the United States Government nor the University of California nor any of their employees, makes any warranty, express or implied, or assumes any legal liability or responsibility for the accuracy, completeness, or usefulness of any information, apparatus, product, or process disclosed, or represents that its use would not infringe privately owned rights. Reference herein to any specific commercial product, process, or service by trade name, trademark, manufacturer, or otherwise, does not necessarily constitute or imply its endorsement, recommendation, or favoring by the United States Government or the University of California. The views and opinions of authors expressed herein do not necessarily state or reflect those of the United States Government or the University of California, and shall not be used for advertising or product endorsement purposes.

Femtosecond Laser Materials Processing

B C Stuart, P S Banks, M D Perry, M D Feit, R S Lee,
F Roeske, J P Armstrong, H T Nguyen, J A Sefcik

Lawrence Livermore National Laboratory
P O Box 808, L-439, Livermore, CA 94550

Keywords laser processing, machining, ablation, femtosecond/subpicosecond laser pulses, high explosives

ABSTRACT

Femtosecond lasers enable materials processing of most any material with extremely high precision and negligible shock or thermal loading to the surrounding area. Applications ranging from drilling teeth to cutting explosives to making high-aspect ratio cuts in metals with no heat-affected zone are made possible by this technology. For material removal at reasonable rates, we developed a fully computer-controlled 15-Watt average power, 100-fs laser machining system.

1. INTRODUCTION

The use of femtosecond lasers allows materials processing of practically any material with extremely high precision and minimal collateral damage. Advantages over conventional laser machining (using pulses longer than a few tens of picoseconds) are realized by depositing the laser energy into the electrons of the material on a time scale short compared to the transfer time of this energy to the bulk of the material (either electron-phonon coupling or thermal diffusion), resulting in increased ablation efficiency and negligible shock or thermal stress. We present several examples here, including drilling of teeth, machining of high-explosives, and drilling and cutting of metals, which demonstrate the benefits of, and in many cases are enabled by, using the technology of femtosecond laser materials processing. This is a very active area of research and more information and examples can be found in Refs 1-5, and references therein.

The physical nature of the short-pulse laser interaction with material (along with the benefits) results in only a very thin layer ($\approx 0.1\text{-}1\ \mu\text{m}$) of material being ablated by each pulse. For efficient bulk material removal, laser systems of high repetition rate and high average power are necessary. In addition, for femtosecond laser materials processing to gain industrial acceptance, the laser systems must be made turn-key and reliable. We have taken a step in that direction by

constructing a computer controlled, 15-W average power system that requires no laser knowledge or adjustments on the part of the operator

2. DIELECTRICS

In transparent dielectric materials irradiated with high-intensity femtosecond pulses, initial free electrons are produced by multiphoton ionization. These electrons are accelerated in the laser field and produce additional free electrons by collisional ionization. The relative ratio of the two mechanisms is pulse width dependent. A critical density plasma ($\approx 10^{21} \text{ cm}^{-3}$ @ 1053 nm) is formed in a thin layer ($\approx 1 \mu\text{m}$) at the surface of the dielectric and ablation occurs by expansion of the $\approx 10 \text{ eV}$ plasma away from the surface. Very little energy (shock or thermal) is coupled into the bulk material because the pulse duration is shorter than the characteristic time for energy transfer from the electrons to the lattice (a few ps for most dielectrics). Measured and calculated ablation thresholds for fused silica⁶ are shown in Figure 1 over a wide range of pulse duration. The deviation from $\tau^{1/2}$ scaling at $\approx 20 \text{ ps}$ signals the transition into this new regime of nonthermal ablation. We also include measurements by Kautek, et al⁷, in glass down to 20 fs. The continuously decreasing threshold for shorter pulses means that less energy is coupled into surrounding areas as shock or thermal loading. As the pulse duration becomes extremely short, there is no time for an avalanche to occur and multiphoton ionization alone produces the critical density plasma.

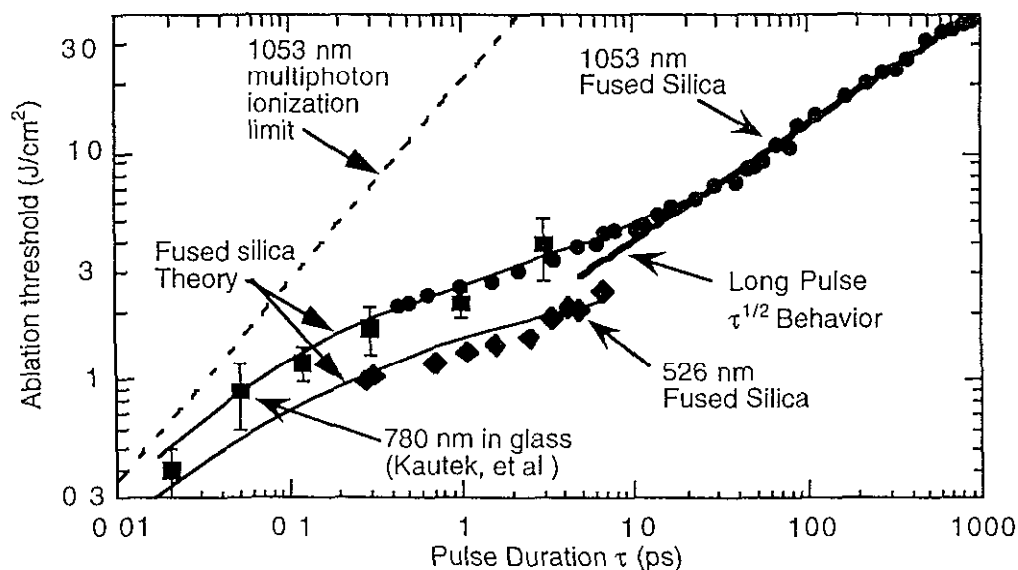


Figure 1 Measured (\bullet fused silica 1053 nm, \blacklozenge fused silica 526 nm, \blacksquare glass⁷ 780 nm) and calculated (solid line) ablation threshold. Deviation from $\tau^{1/2}$ scaling below 20 ps indicates the new regime of nonthermal ablation. The calculated threshold for ablation by multiphoton ionization alone (reaching critical density) is indicated.

From the standpoint of this mechanism of laser interaction, enamel, bone, etc are simply dielectrics and exhibit the same behavior as materials examined in initial experiments (SiO_2 , CaF_2 , etc) Shown in Figure 2 are electron micrographs of the surface of a tooth following material removal by 14-ns laser pulses and 350-fs pulses The pulses are produced by a variable pulse duration laser operating at 1053 nm and 10 Hz Cracking of the surrounding material and the uncontrollable nature of material removal by thermal shock are readily apparent in the enamel irradiated by nanosecond pulses (Fig 2a) In this regime, linear absorption due to defects produces inhomogeneous energy absorption across the laser beam and thermal stresses build up causing ablation first from the point with the least material strength This is not the case with femtosecond pulses where all regions throughout the laser beam profile with sufficient intensity for multiphoton ionization will be removed resulting in extremely fine control of the position of material removal (Fig 2b) In addition, the morphology in the femtosecond case is characteristic of internal enamel and there is no evidence of heat transfer into the surrounding material

This non-thermal material removal mechanism results in a minimal increase in temperature of the surrounding material Thermal measurements show that when irradiated with 500 conventional 1-ns laser pulses, the bulk temperature of a 1-mm slice of tooth increased by over 40 °C while for femtosecond pulses the temperature rise was less than 2 °C (Figure 3) The fluence in each case was set to remove approximately 1 μm depth of material per pulse This required 30 J/cm^2 for the ns pulses and only 3 J/cm^2 for the fs pulses The practical consequences in dentistry are substantial In the case of existing laser systems, active cooling of the tooth is necessary to prevent permanent damage to the pulp (5°C increase) while no cooling would be necessary with femtosecond laser pulses

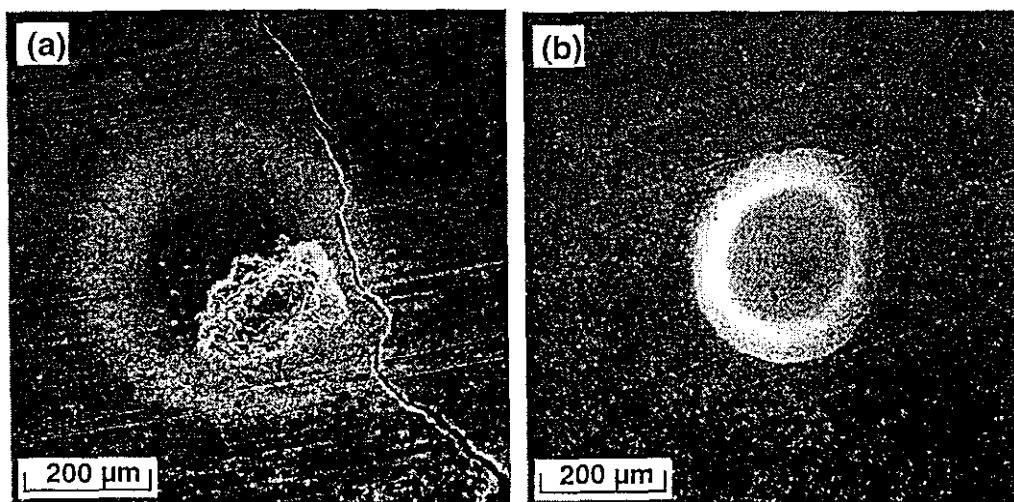


Figure 2 (a) Drilling of enamel with 14 ns, 30 J/cm^2 laser pulses Enamel is removed by a conventional thermal/fracture mechanism resulting in cracking and collateral damage from temperature rise and thermal shock (b) Drilling of enamel with 350 fs, 3 J/cm^2 laser pulses Enamel is removed by a nonthermal mechanism which eliminates collateral damage and leaves the surface in its natural state

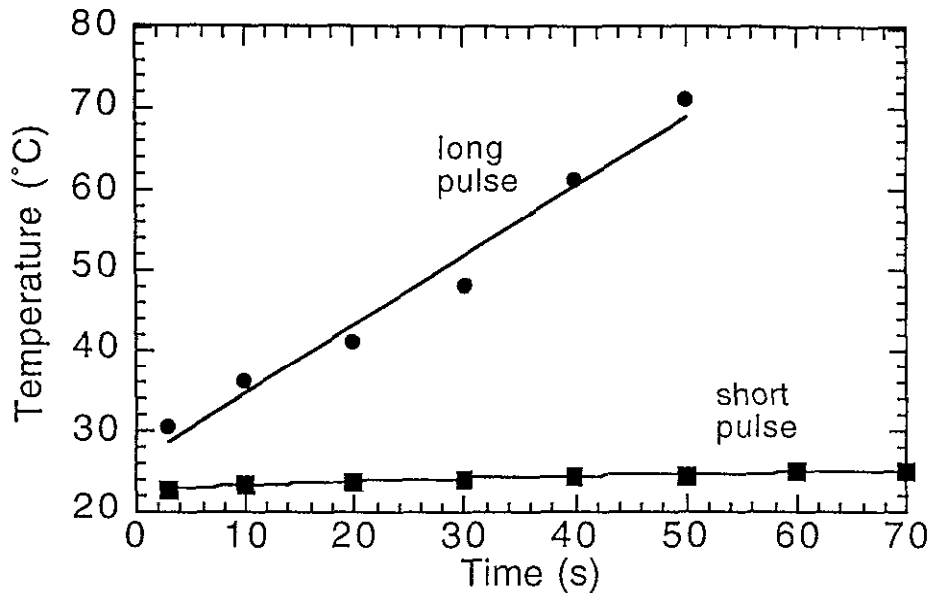


Figure 3 Temperature increase of bulk tooth due to drilling with nanosecond (circles) and femtosecond (squares) laser pulses. In both cases, the laser wavelength was 1053 nm and the material removal rate was 1 $\mu\text{m}/\text{pulse}$ at 10 Hz.

3. HIGH EXPLOSIVES

Another class of dielectric materials that greatly benefit from the reduced thermal and shock loading during femtosecond laser machining is that of high explosives (HE). Cutting and machining operations on energetic materials present significant safety challenges. If conventional machine tools are used, improper fixturing of the work, improper tool configuration and improper cutting speeds have resulted in violent reactions during machining operations. In addition, significant hazardous waste is generated from the machining chips and the necessity of using cutting fluids to cool the cutting tool. Ablation of high explosives by femtosecond laser pulses offers an attractive alternative to conventional machining. Absorption of these ultra-short pulses occurs on such a short time scale that the material is ablated with virtually no heat transfer to the surrounding material, resulting in a "cold" laser cutting process. Additionally, the shock wave accompanying femtosecond ablation decays to low levels after a depth of $\approx 1 \mu\text{m}$. The waste products from short-pulse laser cutting are, for the most part, solid carbon or benign gases, which can be released into the atmosphere. If the quantity of chlorine and fluorine from the binder is a problem, these gases are easily removed.

We used LX-16 explosive (96%PETN/4% FPC 461 binder) for our initial experiments because PETN is one of the most sensitive of the secondary explosives. In some of the experiments the beam first cut through the HE pellet and then into a stainless steel substrate and in other

experiments the beam first cut through stainless steel and then into the HE pellet. In either case, no reaction was observed in the LX-16 pellets. We also cut through pellets that were not backed by a substrate. Figure 4a shows two cuts across a 6-mm diameter, 2-mm thick pellet made using a 1-kHz, 100-fs Ti sapphire CPA laser system. In addition to LX-16 we cut pellets of LX-14 (95.5% HMX/4.5% Estane), LX-15 (95% HNS/5% Kel-F), LX-17 (92.5% TATB/7.5% Kel-F), PBX-9407 (94% RDX/6% Exon 461), and pressed TNT.

Fourier Transform Infrared Spectroscopy of the laser cut LX-16 surface showed no evidence of any chemical reaction products. The laser cut surface was chemically identical to the original LX-16 material. The ablation process is also very efficient in explosives with several microns of material being removed per pulse. We also observed for small spot sizes (approximately 25 μm) that after an initial taper, the cut would exhibit extremely straight walls extending for several millimeters. This enables cuts with extremely high aspect ratios of 1000:1 and more.

The only experiment in which reaction was observed was in cutting a LX-16 pellet when we did not compress the pulse after amplification (a factor of 5000 increase in pulse length). Using 500-ps pulses at a power level high enough to remove material, ignition of the LX-16 was observed. Examination of the pellet afterward revealed that the edges of the cut were melted and contained a multitude of reaction products (Fig. 4b). In another series of experiments to drill through a 1-cm thick sample, 3-ps pulses penetrated only 3 mm after 30 seconds, whereas 120-fs pulses went completely through in 2 seconds. It is clear that ultra-short pulses are essential to laser cutting and machining of energetic materials.

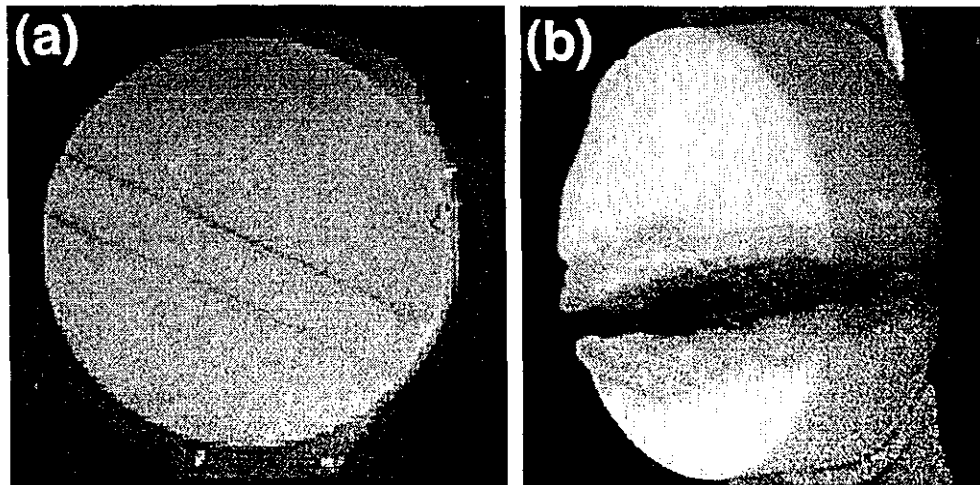


Figure 4. Cuts in explosive pellet (PETN) by (a) short pulse and (b) long pulse laser. Thermal deposition in the long-pulse case caused the pellet to ignite.

4. METALS

In metals, by choosing the laser pulse duration such that the thermal penetration depth is on the order of the optical skin depth, very small amounts of material ($0.01\text{--}1\ \mu\text{m}$) can be precisely removed with minimal transport of energy by either shock or thermal conduction away from the volume of interest. The vaporized material hydrodynamically expands from the surface with little energy deposited in the bulk and no melt stage. Thus, there is no heat-affected zone in the remaining bulk material nor recast layer. Figure 5 shows the cross-section of a $400\text{-}\mu\text{m}$ hole in $750\ \mu\text{m}$ thick stainless steel at 45° , the metallic grain structure is unaltered up to the edge of the cut. The top (entrance) of this cut is shown in Fig. 6, again with no evidence of slag or heat-affected zone.

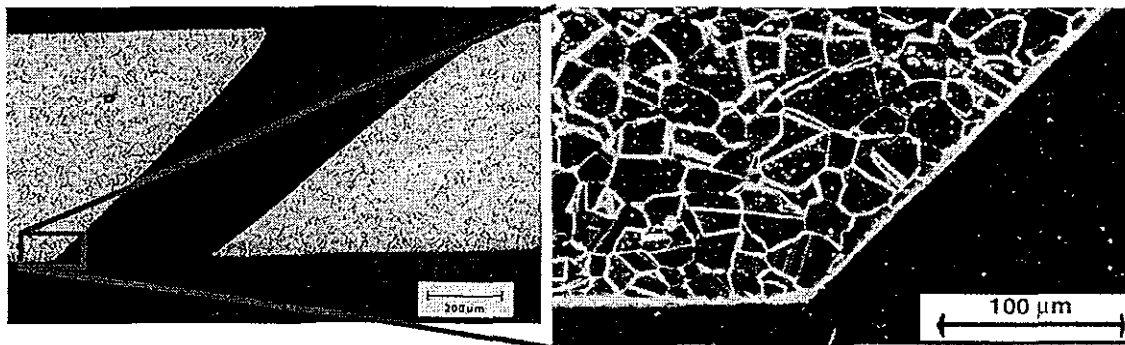


Figure 5 Cross section of hole drilled in stainless steel with 120-fs pulses at 1 kHz

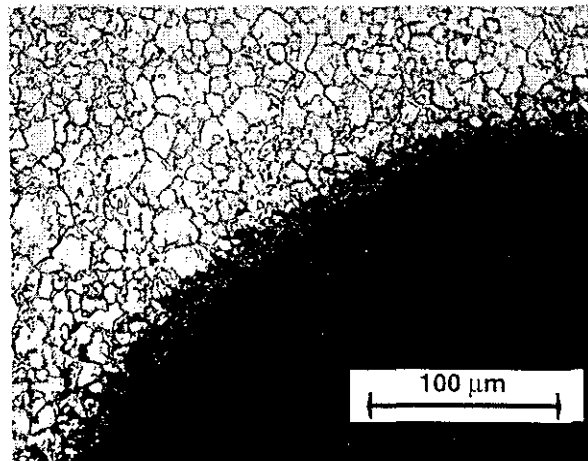
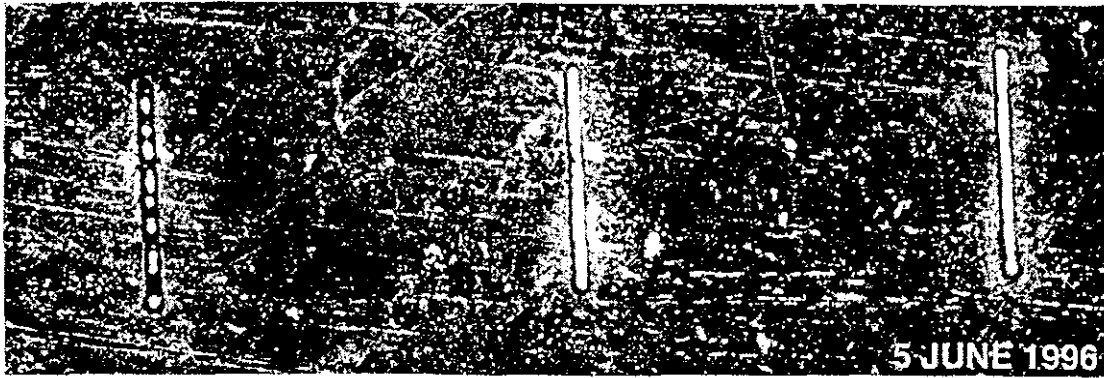


Figure 6 Top of hole drilled in stainless steel. There is no evidence of melting or slag.



Linearly polarized (vert)

Circularly polarized

Linearly pol. (hor)

Figure 7 Three cuts in 140- μm thick stainless steel under identical conditions except for a change in the laser polarization Cuts with the electric field perpendicular to the cutting direction are cleaner

Polarization of the laser also plays an important role in the ablation process, affecting both cut quality and rate Figure 7 shows cuts through 140- μm stainless steel under identical conditions, except the laser polarization is varied from linear parallel to the cut to circular to linear perpendicular to the cut (left to right) Increased light absorption with the electric field pointing into the walls of the metal leads to higher efficiency and cleaner cuts This effect can be understood in terms of Joule heating due to currents induced in the optical skin depth

Figure 8 helps to answer the question of how short a pulse duration is short enough Here, we compare the time to drill through various thicknesses of stainless steel as a function of pulse duration Each was irradiated at 1 kHz, 825 nm, and a fluence of 12 J/cm² with a line focus 50 μm wide In cutting through samples thicker than ≈ 1 mm, it is advantageous to use pulse durations below 1 ps

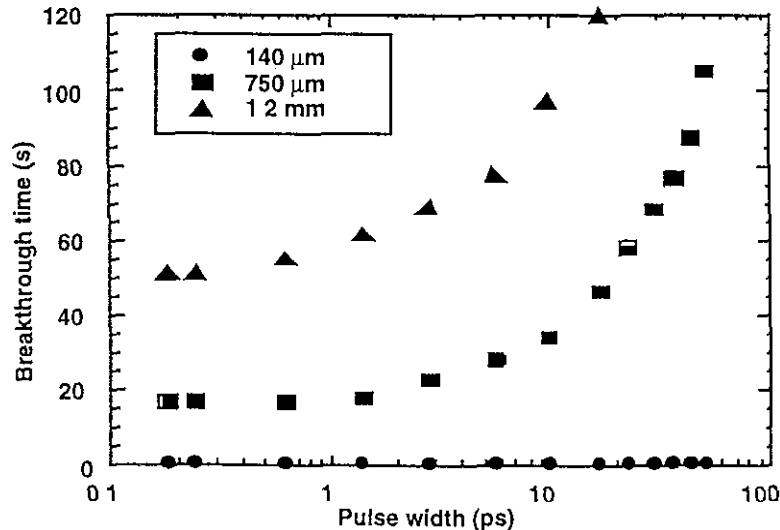


Figure 8 Time to drill through different thicknesses of stainless steel as a function of laser pulse duration

5. 15-W SHORT-PULSE LASER PROCESSING SYSTEM

The rate of material removal scales essentially linearly with the average power of the laser system. We have recently completed a high average power short-pulse laser system for use in an industrial environment. The system is fully computer-controlled and is designed to be run by a machine-tool operator. A block diagram of the system is shown in Fig 9. It is based on conventional technology, i.e. arc-lamp pumped, intracavity-doubled Nd YAG pumping Ti sapphire, and was designed to operate without the added complexity of cryogenic cooling of the Ti sapphire crystals.

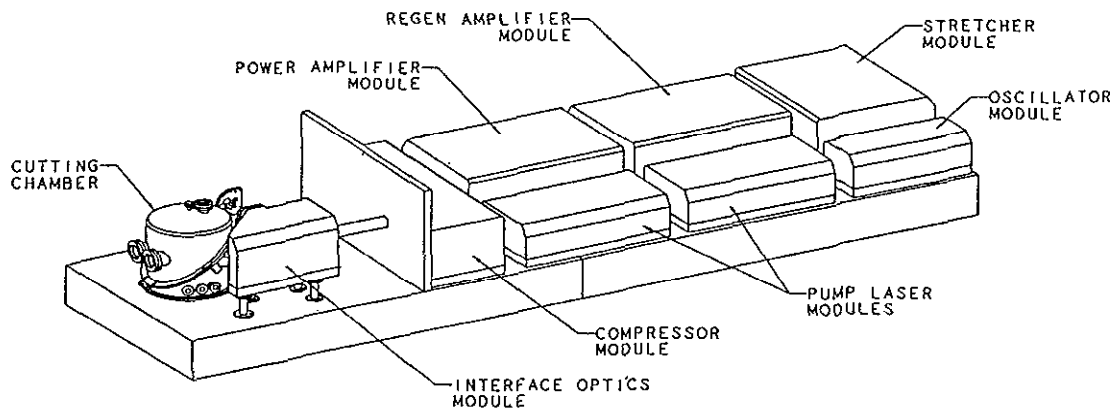


Figure 9 Configuration of 15-W short-pulse machining system

The system begins with a turn-key, Kerr-lens mode-locked Ti sapphire oscillator (Coherent Vitesse) which produces 90-fs pulses at 810 nm. These pulses are stretched to 500 ps in a four-element all-reflective stretcher before being amplified in a regenerative amplifier followed by a power amplifier. Each amplifier is pumped by approximately 80 W at 10 kHz in two beams. Each pump leg is generated by intracavity doubling (LBO) of a single arc-lamp pumped Nd YAG head. Up to 100 W average power at 532 nm is available from each module, but the power delivered to the Ti sapphire crystal is derated and regulated by a waveplate/polarizer combination to compensate for lamp aging. The regenerative amplifier produces 9 W and the power amplifier 22 W. Each was designed to compensate for the very strong thermal lens induced by the high average power pumping in a small spot size. After compression the output power is up to 15 W (1.5 mJ @ 10 kHz) in 100-fs pulses. The system is separated into modules, with each beam input to each module actively computer-controlled to maintain alignment. The compressed pulses are directed into a cutting chamber through an interface optics module, which contains the final focusing lens and active beam control to keep the laser aligned to the work piece.

5. ACKNOWLEDGMENTS

The authors thank all those involved in the design and construction the fully-integrated 15-W laser system. This work was performed under the auspices of the U S Department of Energy by Lawrence Livermore National Laboratory under contract No W-7405-ENG-48

6. REFERENCES

- 1 S Nolte, C Momma, H Jacobs, A Tünnermann, B N Chichkov, B Wellegehausen, and H Welling, "Ablation of metals by ultrashort laser pulses", *J Opt Soc Amer* **B14**, pp 2716-2722, 1997
- 2 B C Stuart, M D Perry, M D Feit, L B Da Silva, A M Rubenchik, J Neev, "Machining of biological materials, dielectrics, and metals with femtosecond lasers", *OSA TOPS on Lasers and Optics for Manufacturing*, Andrew C Tam (ed), Vol 9, pp 94-98, 1997
- 3 H Varel, D Ashkenasi, A Rosenfeld, M Wahmer, E E B Campbell, "Micromachining of quartz with ultrashort laser pulses", *Appl Phys* **A65**, pp 367-373, 1997
- 4 X Liu, D Du, G Mourou, "Laser ablation and micromachining with ultrashort laser pulses", *IEEE J Quantum Elect* **33**, pp 1706-1716, 1997
- 5 F H Loesel, M H Niemz, J F Bille, T Juhasz, "Laser-induced optical breakdown on hard and soft tissues and its dependence on the pulse duration-experiment and model", *IEEE J Quantum Elect* **32**, pp 1717-1722, 1996
- 6 B C Stuart, M D Feit, A M Rubenchik, B W Shore, and M D Perry, "Laser-induced damage in dielectrics with nanosecond to subpicosecond pulses", *Phys Rev Lett* **74**, pp 2248-2251, 1995
- 7 W Kautek, J Kruger, M Lenzner, S Sartania, C Spielmann, F Krausz, "Laser ablation of dielectrics with pulse durations between 20 fs and 3 ps", *Appl Phys Lett* **69**, pp 3146-3148, 1996

Technical Information Department • Lawrence Livermore National Laboratory
University of California • Livermore, California 94551

